INVESTIGATIONS ABOUT THE ACCURACY OF TARGET MEASUREMENT FOR DEFORMATION MONITORING

Mario Alba, Fabio Roncoroni, Marco Scaioni

Politecnico di Milano, DIIAR, Polo Regionale di Lecco, via M. d'Oggiono 18/a, 23900 Lecco, Italy - (mario.alba, fabio.roncoroni, marco.scaioni)@polimi.it

Commission V, WG V/3

KEY WORDS: Laser scanning, Calibration, Accuracy analysis, Deformation, Civil engineering, Retro-reflecting target

ABSTRACT:

Experience in applications of TLS for deformation monitoring of concrete structures have shown the need of further exhaustive study about the quality of retro-reflecting target measurement. Indeed, this factor is highly influencing the georeferencing that is of primary importance to compare scans acquired at different epochs. Here some tests carried out by means of a RIEGL LMS-Z420*i* laser scanner are reported. In addition, several algorithms for automatic retro-reflecting target measurement have been applied, and new ones proposed. Results obtained from lab experiments have revealed a good repeatability on target measurement, while the accuracy is highly affected by a bias on the measured range. This mainly depends on the distance of the target from TLS, and on the angle of incidence of laser beam. In order to compensate for this error, two approaches have been successfully tested: the estimation of a corrective function, and the use of an algorithm for automatic retro-reflecting target measurement which locally estimates the bias on the range.

1. INTRODUCTION

Terrestrial Laser Scanning (TLS) is today widely used in many application fields, with different capability to satisfy end-user requirements. Broadly speaking, modern instruments (Lemmens, 2007) are highly capable to provide a 3-D geometric reconstruction of objects and surrounding environment through fast acquisition of dense clouds of unspecific points. Several viable strategies can be followed for georeferencing scans captured from different points of view into the same reference frame. Currently these account for the use of *targets* (Valanis & Tsakiri, 2004), *surface matching algorithms* (Akca, 2007), *direct georeferencing* (Gordon & Lichti, 2004), and contemporary *coregistration of images and 3-Dviews*.

More complex is the information extraction task. In all cases where surfaces can be modelled by elementary geometric primitives, the process of object reconstruction can be completed in an almost automatic way. This happens when natural surfaces (e.g. ground, rock faces, water basins, open pit mines) have to be reconstructed by TIN models, or regular shapes have to be fit into data (e.g. in modeling of industrial plants). In the cultural heritage field, much work is still to do in object modeling, despite of the amount of information stored in laser scanner data (Fassi, 2007).

Recently the number of people interesting in application of TLS for deformation monitoring is quickly increasing. This is motivated by the fact that this technique would allow to analyse deformations of whole surfaces instead of single points, like current monitoring geodetic and photogrammetric systems do. Common requirements of these applications are: (i) the high accuracy and point density; (ii) the registration of all adopted scans at different epochs into the same reference frame in order to detect changes of the object shape. So far, the former issue has been coped with in different ways, which however always try to exploit the redundant observations to reduce the effect of measurement errors in surface reconstruction. Approach to do this are based on fitting object surfaces to a set of several planar patches (Lindembergh & Pfeifer, 2005), or by interpolating the whole surface with a regular geometric shape, if possible (Schneider, 2006; Van Gosliga *et al.*, 2006). In case irregular surfaces have to be compared, the use of *surface matching algorithms* can be adopted to detect local deformation (Monserrat & Crosetto, 2008). The latter problem might concern manifold aspects, related to the size of the object under investigation, the portion of the object which may change its shape and the presence of stable the period and the frequency of measurements, the need of registering these into a given external reference frame, for example referred to the local plumb line. In general, the widespread solution to define a permanent reference frame common to several scans taken at diverse epochs is based on *retro-reflective targets* (RRT).

During some experimental tests of deformation monitoring of civil engineering structures, the demand of exhaustive study about the precision of this kind of targets has arisen, being this factor highly influencing the quality of georeferencing that is of primary importance to compare scans acquired at different epochs. Because this subject has been poorly investigated so far, some experimental tests have been carried out to this aim.

The paper is organized on a preliminary decription of RRTs and their use in common TLS practise (Sec. 2). In section 3, the experimental tests that have been leaded is described. Data analysis and presentation of the outline problems, as well as the proposed solution, is the subject of section 4; here also a comparative review of the algorithm which are usually adopted for the automatic measurement of RRTs is reported. Finally, conclusions and further developments are drawn in section 5.

2. RETRO-REFLECTIVE TARGET OVERVIEW

The use of RRTs for scan registration is a standardized and operational process, which is usually recommended by different instrument vendors. The automatic recognition and measurement of such targets is implemented in several terrestrial laser scanners and in their companion data processing softwares. Instruments are capable to make a preliminary localization of the rough target position, and consequently a high resolution scanning is performed in the nearby of it. As alternative, the user might manually aim the scanner head towards targets' approximate position, or these can be achieved by a list of point coordinates. This latest solution is worth for monitoring applications, where the same targets are measured at different epochs, and then their rough position is already known. However, strategy and algorithms adopted by specific instruments to carry out RRT measurement is generally unknown, in the knowledge of the authors.

Some instruments can use only targets of a specific material and shape (e.g. Leica); others (Trimble) are capable to work with different kinds of RRTs, but they guarantee the best precision only by using proprietary targets. Finally, other scanners are able to use indifferently RRs featuring other shape (plane, cylindrical, spherical) and size.

For the above-mentioned grounds, a common method to set the best dimension of target as a function of the distance from the instrument stand-point is difficult to be found. On the other hand, some general factors exist which influence the precision of measurement of all ToF scanners:

- the laser beam-width divergence;
- the maximum angular resolution;
- the incidence angle of laser beam on the target surface;
- the target intensity response.

In particular, hereafter some experiences about RRT measurement with the Riegl LMS-Z420*i* laser scanner will be reported. Technical documentation on this ToF long-range instrument can be directly found on the vendor website.

2.1 RR target measurement with Riegl LMS-Z420*i*

The Riegl LMS-Z420*i* laser scanner can be georeferenced on the basis of RR targets, which are used as Ground Control Points (GCP) to compute a 3-D roto-translation from the Intrinsic Reference System (IRS) of each scan to the Ground RS (GRS). During the data collection stage, the approximate coordinates of each RRTt are automatically identified by data acquisition control software Riegl Riscan Pro. This task is accomplished by analysing the points featuring the highest intensity response in a preliminary low-resolution scan. Thank to the non Lambertian behaviour of retro-reflecting materials, laser beams are reflected towards the scanner head with a very high intensity that outstands from the surrounding points. In a second stage, targets are scanned at higher resolution, according to the distance from the scanner. This solution allows it to capture the surface around each target at a higher point density w.r.t. the remaining parts of the object to be scanned. By this approach, the precision of target measurement is improved, and consequently that of georeferencing as well.

From the analysis of several targets captured with LMS-Z420*i* scanner, it is possible to outstand 4 different strategies that are followed for RRT scanning. Parameters influencing the selection of a specific strategy are the *size* (i) of the target and its *distance* (ii) from the sensor. These values are *a priori* available before high-resolution scanning: the former (i) because the user has to select the specific kind of target to be used (shape and dimensions); the latter (ii) it's already known from preliminary low-resolution scanning. First the Riegl system scans a squared window (with side D) large about 5 times the largest dimension d of the target around its approximate location whit a resolution that depends on the distance. From this step on, different strategies are applied:

1. *up to about 4 m*: the TLS scans the window whit a grid of 100×100 points, resulting in a horizontal and vertical spatial grid resolutions of:

$$s_H = s_V = D/100 \approx d/20 \quad (1)$$

2. *from 4 to 32 m*: the horizontal scan resolution is selected as in the previous case 1; in the vertical direction, the surface is scanned at the maximum angular (and then spatial) resolution;
3. *from 32 to 60 m*: the system adopts a scan window at the maximum angular resolutions in both directions;,
4. *over 60 m*: a grid of 65×65 points is scanned at the maximum angular resolution, disregarding the target size. Obviously, the dimensions of the scan window increases with a fix proportion w.r.t. to the range.

This strategy has been implemented to assure a correct scanning of target windows in common practitioner applications, where accuracy in surface reconstruction of a few cm is enough (e.g. in open pit surveys). In special applications for deformation monitoring, where a higher accuracy in georeferencing is needed, the size of the target must be accurately selected according to the strategy that will be applied to perform its measurement. In particular, the size of the target should not exceed the scan window size, otherwise it would not be possible to detect the target centre. On the contrary, if the target size is too small, this would be measured with a not sufficient number of points. The same should be checked out by analysing the laser footprint.

3. DESCRIPTION OF EXPERIMENTS

In this section we will give a presentation of different tests carried out by means of a Riegl LMS-Z420*i* laser scanner in order to assess problems in the measurement of RRTs. Here the target search and scanning has been performed by using the data acquisition control software Riscan Pro.

3.1 Test 1: long-range measurements

The first test has been carried out to evaluate the precision of target measurement according to different ranges from sensor-to-object, up to 300 m. Influence of laser beam angle of incidence, laser footprint, and type and dimension of RRTs are analysed. The measurements have been carried out in an outdoor site due to the required long-range.

During the first test a timber frame of 1×2 m has been adopted, where 11 targets of different size and shape covered by retro-reflecting paper have been fixed. All targets can be grouped into the following 3 categories:

1. *square foil* with 4 cm (no. 8), 5 cm (no. 4), and 6 cm (no. 1,3,9,11) side;
2. *circular foil* with 10, 20 and 30 cm diameter (no.2,5,6, respectively);

3. *aluminium disk* (Φ=12 cm) with a central reflecting circular surface of 10 cm and a thickness of 0.5 cm (no. 7);
4. *aluminium disk* (Φ=8 cm) of dark colour with a central reflecting circular surface of 3.5 cm and a thickness of 0.3 cm (no. 10).

The 3-D coordinates of target centres have been measured by a total station Leica TCA2003 into the GRS; results have shown a std.dev less than ±0.4 mm.

During this test, the scanner Riegl LMS-Z420*i* has been positioned on a fixed stand-point and the target framework has been moved along the range direction at different distances (10, 50, 100, 200 and 300 m). At each distance step the panel has been rotated of 30 deg w.r.t. the vertical plane (configuration "v30"), and of 30 and 45 deg w.r.t. the horizontal plane ("h30" and "h45"). Estimated accuracy of these rotations is in the order of ±4 deg. The whole framework has been scanned at the maximum angular resolution (0.004 gon) and the target have been recognized, scanned and measured by Riscan Pro software.

3.2 Test 2: close-range measurements

The second group of tests has been setup to evaluate systematic errors in range (r), horizontal (φ) and vertical (θ) angles corresponding to the measured target centres. In a 12×6×3 m room of the Politecnico di Milano university, 38 square RRTs of size 5 cm have been glued on the walls and measured by a total station Leica TCRA1200 whit a std.dev less than ±1mm. To distinguish between two different tests that have been carried out, these have been referred to:

- *Ex2.1*: the laser scanner has been positioned in a central stand-point (n. 300 in Figure 1) and 9 scans have been repeated for each target in order to check the repeatability;

- *Ex2.2*: the laser scanner has been positioned over two stand-points (n. 100 and 200 in Figure 1) at a relative distance of ~7 m. From each stand-point, 3 different scans rotated in the horizontal plane of 120 deg have been captured.

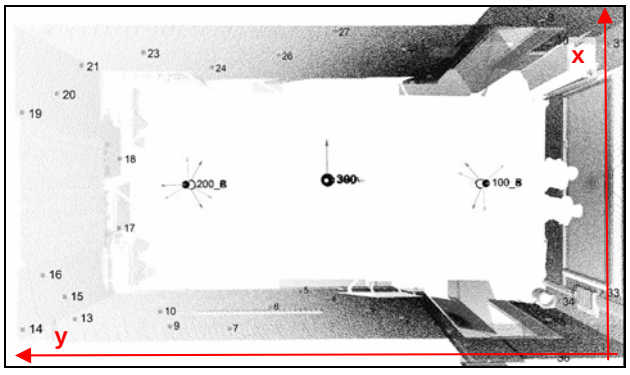

Figure 1. The room of Test 2 with TLS stand-points and target positions for both Ex2.1 and Ex2.2

3.3 Test 3: Error modeling

The last test has been setup to evaluate the precision of target measurement in relation to laser beam angle of incidence and range. In this case a square RRTs of side 5 cm has been glued in the centre of a circular laminate (Figure 2) that can rotate around both vertical and horizontal axes without changing the target's centre position. The target was scanned using the automatic procedure implemented in Riscan Pro software.

The range of measurement was selected in function of the algorithm adopted by Riscan Pro to scan the target, as described in sub-section 2.1. In the considered range (4-35 m) and for a target size d=5 cm, the horizontal spatial resolution is given by $s_H \approx d/20$=2.5 mm, while the vertical resolution s_V always depends on the maximum angular scan resolution. The size of the scan window is about 23×23 cm. The following tests have been performed:

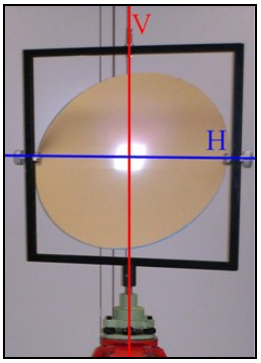

Figure 2. Target with its rotation axes

- *Ex3.1*: the target has been scanned at every 0.3 m distance step from 4 to 20, and from 20 to 35 m at 1 m steps. The frame has been oriented to face the scanner;

- *Ex3.2*: the target has been placed at distances of 9, 13.5 and 18 m from the scanner, and rotated of 10 deg steps from -70 to 70 deg w.r.t. the vertical and horizontal target's axes, with an accuracy of about ±1 deg. In addition, for the range of 13.5 m the target has been also simultaneously rotated in both directions. This has resulted in 3-D incidence angles (estimated std.dev ±0.01°) of 18.5, 31.4, 47.6, 61.3, 75.5, 85.6 deg.

4. ANALYSIS OF RESULTS

4.1 Algorithms for automatic RR target measurement

When a target is scanned, the acquisition software calculate automatically the centre of it by applying an alghoritm for its measurement. Nevertheless, the algorithms implemented in commercial softwares are unknown for the most.

In Lichti *et al.* (2000) three different methods are described. The first defines the centre of each target as the position with the maximum radiance. The second defines the centre by the mean position of the radiometric centre of the 4 strongest returns. The third algorithm defines the centre of the target as the radiometric centre of all returns. These methods will be referred to henceforth as "maxrad", "maxrad4" and "radcent".

In Valanis & Tsakiri (2004) some other algorithms are presented and tested using a Cyrax 2500 TLS in laboratory conditions. The method used was based on the *fuzzy clustering* technique introduced by Bezdek (1981). In the present work, results obtained by an algorithm based on the same method ("fuzzypos") will be presented, even though it has been modified to work with RRTs adopted in tests described in Sec.

3. This algorithm starts from the classification of all points of the target into three classes according to their reflectivity. Once the classification is completed, classes are recognized by calculating the mean value of the points that are assigned to each one of them. Finally, the mean position with the largest mean reflectivity values is used. A carefull analysis of several targets measured by "fuzzypos" algorithm has revealed that the parts of the data that correspond to the highly reflective areas of the target are shifted w.r.t. the points whit lower intensity. This finding will be confirmated by other experimental tests described in Par. 4.2.1.

In addition to methods above illustrated, a new algorithm called "intersect" has been designed to reduce the offset error. In a first step the cluster analyses is used to divide all points into three classes. For the class with the lower intensity, which belongs to the background surface around the RRT, a plane π is fitted using a RANSAC technique (Fischler & Bolles, 1981). The gravity centre G of the class with the largest intensity (i.e. the RRT itself) is computed. The target centre T_C is computed as the intersection between π and a vector connecting G to the IRS centre.

All discussed method has been tested on test-field adopted in Test *Ex2.2* (Sub-sec. 3.2), but using only the scan from stand-point 100. Residuals w.r.t. GCP are reported in table 3, which shows that some methods proposed give better results than the proprietary Riscan sofware algorithm ("riscan"), which is unknown. Moreover, the "intersect", "fuzzypos" and "radcent" methods present approximately the same results, while "maxrad" and "maxrad4" have significant flaws. In the second part of the table, std.dev.s of georeferencing parameters computed on the basis of target measurement performed by different algorithms are reported.

Algorithm	**RMSE of 3-D residuals on targets [mm]**	**Estimated georeferencing parameters (σ)**			
		Rotations of IRS [mgon]			***Position of IRS centre [mm]***
		Ω	***Φ***	***K***	
maxrad	12.3	7.2	11.3	6.2	2.7
maxrad4	19.1	19.6	30.6	17.0	4.2
radcent	4.0	6.4	10.0	5.3	0.9
fuzzypos	3.9	6.2	9.6	5.5	0.9
intersect	***3.8***	***6.2***	***9.1***	***5.1***	***0.9***
riscan	5.0	7.7	11.9	6.6	1.1

Table 3. Target residuals after scan georeferencing on GCPs and std.dev.s of georeferencing parameters

4.2 Accuracy and repeatability on RR target measurement

In this section results obtained from different tests have been organized in order to report different outlines and problems which have been observed. At the end, in Sub-sec. 4.3 an empirical model to compensate for errors in range measurement is then proposed, discussed and validated.

4.2.1 Accuracy of target measurement

In Test 1 the coordinate of target centres have been measured by proprietary algorithm of software Riscan Pro ("riscan"). To check the accuracy of their measurement, 6 parameters of a 3-D roto-translation between the Intrinsic RS (IRS) of the laser scanner and the GRS has been computed for all configurations, according to different distances and rotations. Table 4 shows the RMSE after the transformation. In general, the accuracy linearly decreases according to the distance. In this case, different incidence angles do not significantly influence the final results.

The precision of single target declines when the beam footprint is larger than the size of target. Otherwise targets of large dimension have resulted in less accuracy in short range. For example, targets no. 5 and 6 have not given good results as far as a distance of 100 m.

The data acquired do not present systematic error in range, horizontal and vertical angles corresponding to the computed target centre. However, a further problem has been outlined by computing a plane interpolating all points of the framework surface, after removing those points belonging to targets. Afterward, the orthogonal distance from each target centre to the plane has been calculated. The results have been summarized in Figure 5, showing a systematic bias in function of distance, i.e. the target centre has resulted closer to the scanner w.r.t. the interpolating plane. This problem is signed some time in literature (Pfeifer *et. al.*, 2007). The large difference between the behaviour of off-planes at 10 m and the others can be imputed to the strategies adopted by Riscan Pro to scan RRTs.

Framework rotations	**Distance laser scanner-framework [m]**				
	10	***50***	***100***	***200***	***300***
Ortho [mm]	2.8	4.3	5.1	6.2	9.7
v30 [mm]	4.6	3.7	5.6	7.0	n.a.
h30 [mm]	3.4	4.2	5.6	7.5	n.a.
h45 [mm]	3.2	3.9	3.8	8.1	n.a.

Table 4. RMSE of target centres [mm] after roto-translation

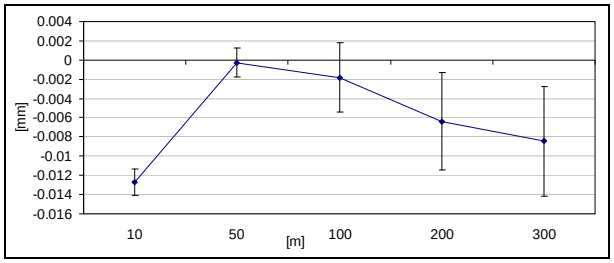

Figure 5. Target off-plane averaged on all targets of Test 1 in function of the distance, with std.dev showing the dispersion of biases

In order to investigate the possible presence of the bias encountered in long-range measurements also in a close-range environment, coordinates of RRTs derived from Test *Ex2.2* have been used. After the computation of a 3-D rototranslation on the set of GCPs (see Sub-sec. 3.2), residuals in X, Y and Z have been computed. As shown in Figure 6, residuals present systematic errors in position, while a better accuracy has been achieved in elevation. Indeed, here the larger residuals on the height of target centres accounts for ±3 mm. The planimetric error fully agrees with the intrinsic accuracy of range measured by Riegl LMS-*Z420i*[1]. This is probably due to the extreme condition of measurement where incidence angles are ranging

[1] According to Lemmens (2007), LMS-Z420*i* features a range accuracy of ±10 mm@50 m, and an angular accuracy of 0.0025 deg (1 σ).

up to 81 gon. However, problems concerning the range measurements on RRTs still occur also for short distances.

Thus, data acquired in Test *Ex3.1* have been used to further study the relation between the offset from coordinate centre of target and the plane fitting the point-cloud of target scan without using the more reflective part.

The specific scan of each target has been exported and processed by the algorithm "intersect" (see Sub-sec. 4.1). Finally the short distance from the gravity centre G of each target and its related background plane π is computed.

The results (Figure 7) presents a growth of the bias as far as a distance of 18 m, then the trend keeps constant and slightly decreases after 28 m. This results is not in disagrement with that obtained in case of long-range distances (Test 1) and summarized in figure 5.

In a second time, data coming from Test *Ex3.2* considering also tilted RRTs have been analysed. Here the coordinate of target centres measured in Riscan software have been used. In each experiment, the coordinate of target in the position facing the TLS have been assumed as reference.

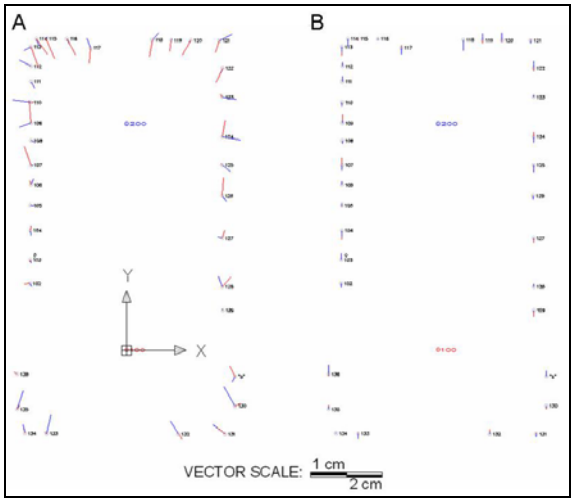

Figure 6. Planimetric (A) and altimetric (B) residuals on targets measured from stand-points 100 (red vectors) and 200 (blue vectors)

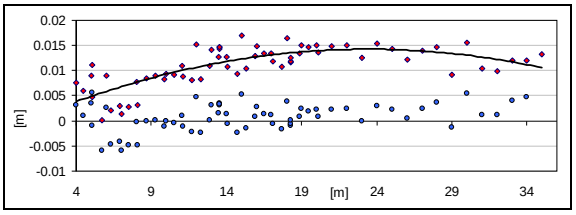

Figure 7. Red points represent arget off-plane in function of the distance, evaluated in close-range field (Test *Ex3.1*). Blue points are residuals after the data interpolation by function (2), which is drawn as black line.

The computed discrepancies between the reference coordinates and those measured in other tilted positions (see table 8) have resulted very small, and only a systematic error in range direction has been outlined. According to this result, the same offset calculated in Test *Ex3.1* has been recomputed. Figure 9 shows that the error in range as function of the incidence angle can be attributed to off-plane bias of each RRT, as confirmed by the high linear correlation (ρ=-0.93) between off-plane bias and error in range.

After the analysis of experiment results, two different ways implemented to reduce the error in range during the RRT measurement will be described in sub-section 4.3.

Rotations		Intensity [0-1]	Range [mm]	Theta [gon]	Phi [gon]	Off-plane bias [mm]
H	*mean*	-0.150	3	-0.003	-0.001	11
	$\pm\sigma$	0.172	5	0.005	0.004	3
V	*mean*	0.000	5	0.002	0.000	10
	$\pm\sigma$	0.001	5	0.006	0.001	3
3-D	*mean*	-0.193	7	0.003	0.001	10
	$\pm\sigma$	0.188	15	0.008	0.003	5

Table 8. Statistics computed on differences between RRTs measured in tilted positions w.r.t. position directly facing the TLS. In rows entitles as "H" and "V", the full set of tilted positions in horizontal and vertical directions are summarized, respectively; in the row named"3-D" contemporary rotations in both directions are considered

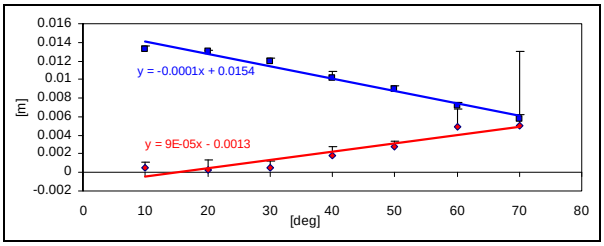

Figure 9. Range error (red) and off-plane bias (bleu) in function of the incidence angle

4.2.2 Analysis of repeatability

In order to evaluate the repeatability of the RR target scanning, the standard deviation of coordinates and other parameter of each target have been computed on the whole set of 9 repeated scans (Test Ex2.1). The RMSE of cartesian coordinate has always resulted less the 1 mm (according to the GRS shown in Figure 5, ±0.6 mm in X and ±0.8 mm in Y and Z). Considering spherical coordinates, RMSE has resulted as ±4.0 and ±9.2 mgon for and angles, respectively, and ±1.1 mm for r. The average number of pixel for each target has been 173, while the RMSE of intensity ±1.4% of the full range. These findings show a very good repeatability of target measurement in a close-range environments, especially if it is compared to that can be obtained from other topographic instruments. Even though only targets at distances under 10 m have been considered here, the results can be extended linearly to a longer ranges.

A second analysis of repeatibility has been carried out by considering data acquired from Test Ex2.2, where 3 different scans rotated of 120 deg have been captured from stand-points 100 and 200. Analysis of absolute residuals w.r.t. GCP coordinates have been already reported in Par. 4.1.1. Here the repeatability of target measurement from the same stand-point (without changing the instrument setup), but with different

initial orientation of the scanner head, has been evaluated in ±4.0 and ±9.2 mgon for φ and θ angles, and ±3.0 mm for r, respectively. These results do not outline very large differences w.r.t. absolute repeatability, considering also the different size of data samples.

4.3 Empirical error propagation modeling

During the data analysis only a systematic error in range direction has been evidenced. Thus, in this sub-section the error is modelled in function of range (4-35 m) and of 3-D incidence angle.

The off-plane bias from the target centre and the plane interpolating the background surface around the RRT is considered as an error in range. In a first step this is modelled only in function of range (r) by means of the following quadratic function:

$$\Delta r_r = K_2 r^2 + K_1 r + K_0 \quad (2)$$

where Δr_r is the correction for the range. Thanks to data coming from Test *Ex3.1*, coefficients of formula (2) have been evaluated as K_0=2·10^{-4} m, K_1=1.2·10^{-3}, and K_2=-3·10^{-5} m^{-1}. After the application of formula (2) to the same data with the computed coefficients, residual errors (see Figure 7) featuring about zero mean, a std.dev of ±2.2 mm, and a maximum absolute value of 5.1 mm have been obtained.

In a second time the error has been modelled in function of 3-D incidence angle (α), by applying the linear correction:

$$\Delta r_\alpha = K_3 r \quad (3)$$

where Δr_α is the correction for the range. Thanks to data coming from Test *Ex3.2*, coefficient of formula (3) has been estimated as K_3=-1·10^{-4} m. After the application of corrections coming from both formulas (2) and (3) to the dataset *Ex3.2*, residuals (see Figure 10) featuring zero mean, a std.dev of ±0.8 mm, and a maximum absolute value of 1.7 mm have been obtained.

The expression for the final corrected range r_c is then given by the sum of both contributes Δr_r and Δr_α:

$$r_c = r + (\Delta r_r + \Delta r_\alpha) \quad (4)$$

To validate the corrective model (4) and the estimated parameters for Riegl LMS-Z420*i* instrument with an independent dataset, measurements taken on RRTs during Test *Ex2.2* have been used. The computed range corrections r_c have been applied to all measured targets, and results compared to GCP reference coordinates. Results have been summarized in table 12, where three algorithms for automatic RRT measurement have been compared: "riscan" algorithm implemented by Riegl Riscan Pro and "fuzzypos" described in Sub-sec. 4.1. Moreover, a modified version of "intersect" algorithm has been applied ("intersect2"), which makes use of the orthogonal distance between background surface and RRT to correct the measured range, instead of using r_c.

In general the estimated range corrections r_c improve the accuracy of georeferencing for both "riscan" and "fuzzypos" algorithms. RMSE on 3-D coordinates of RRTs are better of 16 and 10%, respectively, w.r.t. to non-corrected measurements (compare to table 3). However, even better results have been achieved by using "intersect2" method.

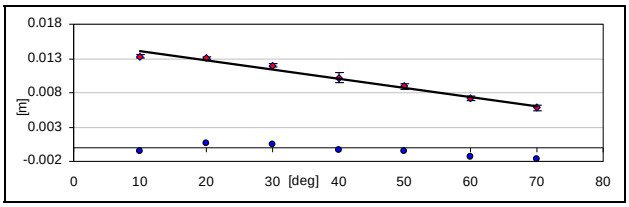

Figure 11. Linear function interpolate the offset plane-point for different 3-D incidence angle. The blue points are the residual on range after correction

Algorithm	RMSE of 3-D residuals on targets [mm]	Estimated georeferencing parameters (σ)			
		Rotations of IRS [mgon]			Position of IRS centre [mm]
		Ω	Φ	K	
intersect2	3.1	5.4	8.2	4.3	0.8
riscan	4.2	6.8	10.7	5.9	0.9
fuzzypos	3.5	5.7	8.9	4.9	0.8

Table 12. Target residuals after scan georeferencing on GCPs and std.dev.s of georeferencing parameters; in this case ranges have been corrected by using model (4)

5. CONCLUSIONS

In the paper different aspects concerning *retro-reflective target* (RRT) measurement by TLS have been analysed. In detail, here the application of Riegl LMS-Z420*i* has been investigated, but results could be extended to other ToF instruments.

Main achievements can be summarized in three items. Firstly, different algorithms for automatic RRT measurement have been compared. Techniques based on point clustering have featured the best, because they are able to take into account differences in range measurements concerning the background surface and the RRT itself. On the other hand, the target size should be properly selected.

Secondly, the repeatibility of RRT measurement is very good (under ±1 mm), property that can be exploited in monitoring applications where the TLS can be accurately repositioned (or kept stable) on the same stand-point. The use of a steal pillar is recommended.

Thirdly, all tests have shown a systematic error in range measurement. This is for the most part due to the range TLS-RRT, and to the 3-D incidence angle. Modelling of this error has allowed to improve the accuracy of georeferencing up to 10-16%, depending on the algorithm adopted for target measurement. Alternatively, good results can be achieved by

using a proposed algorithm for target measurement which directly evaluates the local range correction.

However, the georeferencing based on RRTs is always error-affected, and systematic effects cannot be completely removed. Strategies for reducing error propagation should be always followed in deformation monitoring applications, such as stationing the laser scanner in the same position, and avoiding to place RRT too far from the object to be controlled.

REFERENCES

Acka, D., 2007. Matching of 3D Surfaces and their intensities. ISPRS JPRS, Vol. 62(2), pp. 112-121.

Bezdek, J.C., 1981. Pattern Recognition with Fuzzy Objective Function Algorithms. Plenum Press, New York.

Fassi, F., 2007. 3D modeling of complex architecture integrating different techniques - a critical overview. IAPRSSIS, Vol. 36/5W47, pp. 8, on CDROM.

Fischler, M.A., and R.C. Bolles, 1981. Random Sample Consensus: A Paradigm for Model Fitting with Applications to Image Analysis and Automated Cartography. Comm. ACM, Vol. 24, pp. 381-395.

Gordon, S.J., and D.D. Lichti, 2004. Terrestrial laser scanners with a narrow field of view: the effect on 3D resection solutions. Survey Review, Vol. 37(292), pp. 22.

Lemmens, 2007. Terrestrial Laser Scanners. GIM International, Vol 21(8), pp. 41-45.

Lindenbergh, R. and N. Pfeifer, 2005. A statistical deformation analysis of two epochs of terrestrial laser data of a lock. In: A. Grün, H. Kahmen (ed.s), Opt.3-D Meas.Tech.VII, Vienna, Austria, pp. 61-70.

Monserrat, O. and M. Crosetto, 2008. Deformation measurement using terrestrial laser scanning data and least squares 3D surface matching. ISPRSJPRS, Vol. 63(1), pp. 142-154.

Pfeifer, N., Dorninger, P., Haring, A., and F. Hongchao, 2007. Investigating Terrestrial Laser Scanning Intensity Data: Quality and Functional Relations. In: A. Grün, H. Kahmen (ed.s), Opt.3-D Meas.Tech.VIII,, Zurich, Switzerland, pp. 328-337.

Riegl, http://www.riegl.com (last accessed on 6th May 2008).

Schneider, D., 2006. Terrestrial laser scanner for area based deformation analysis of towers and water dams. Proc. of 3rd IAG Symp. of "Geodesy for Geotechnical and Structural Engineering" and 12th FIG Symp. on "Deformation Measurements", Baden, Austria, 22-24 May, 6 pp., on CDROM.

Valanis, A., and M. Tsakiri, 2004. Automatic Target Identification for Laser Scanners. IAPRSSIS, Vol. 34/5, pp. 1-6.

Van Gosliga, R., Lindenbergh, R., and N. Pfeifer, 2006. Deformation analysis of a bored tunnel by means of terrestrial laser scanning. IAPRSSIS, Vol. 36/5, pp. 167-172.